

Color Dipole Picture at Low-x DIS: The Mass Range of Active Photon Fluctuations

Masaaki Kuroda*

Center for Liberal Arts, Meiji Gakuin University, Yokohama, Japan

Dieter Schildknecht†

Fakultät für Physik, Universität Bielefeld,
Universitätsstraße 25, D-33615 Bielefeld, Germany
and

Max-Planck-Institut für Physik (Werner-Heisenberg-Institut),
Föhringer Ring 6, D-80805 München, Germany

We investigate the mass range of the quark-antiquark fluctuations of the photon that are active in producing the total photoabsorption cross section in the color dipole picture, emphasizing the notions of color transparency and saturation. We consider the implications of measurements at future extensions of the available electron-proton-scattering energy.

I. INTRODUCTION

Deep inelastic scattering (DIS) of electrons on protons at low values of the Bjorken variable $x \cong Q^2/W^2 \lesssim 0.1$ (where Q^2 refers to the photon virtuality and W to the photon-proton center-of-mass energy) is a two-step process: transition, or fluctuation in modern jargon, of the photon into on-shell quark-antiquark ($q\bar{q}$) states, $\gamma^* \rightarrow q\bar{q}$, of mass $M_{q\bar{q}}$, and subsequent scattering of these states on the proton. In terms of the photon-proton (virtual) forward Compton scattering amplitude, the $q\bar{q}$ states interact with the proton via (color) gauge-invariant two-gluon exchange: the color dipole picture (CDP)¹. A model-independent analysis² [1] shows that the photoabsorption cross section, $\sigma_{\gamma^*p}(W^2, Q^2)$, depends on the low-x scaling variable $\eta(W^2, Q^2) = (Q^2 + m_0^2)/\Lambda_{sat}^2(W^2)$ via $\sigma_{\gamma^*p}(W^2, Q^2) = \sigma_{\gamma^*p}(\eta(W^2, Q^2)) \sim 1/\eta(W^2, Q^2)$ for $\eta(W^2, Q^2) \gtrsim 1$ (“color transparency”), while $\sigma_{\gamma^*p}(W^2, Q^2) = \sigma_{\gamma^*p}(\eta(W^2, Q^2)) \sim \ln(1/\eta(W^2, Q^2))$ (“saturation”) for $\eta(W^2, Q^2) \lesssim 1$ ³. The “saturation scale” $\Lambda_{sat}^2(W^2)$ increases with a small power of W^2 , and m_0 is a constant mass, in the case of light quarks somewhat below the ρ^0 -meson mass. Any specific parameter-dependent ansatz [1, 2] for the $q\bar{q}$ -dipole-proton cross section has to interpolate between the $1/\eta(W^2, Q^2)$ and the $\ln(1/\eta(W^2, Q^2))$ dependence.

Based on life-time arguments for $q\bar{q}$ transitions of the photon, $\gamma^* \rightarrow q\bar{q}$, the validity of the CDP requires an

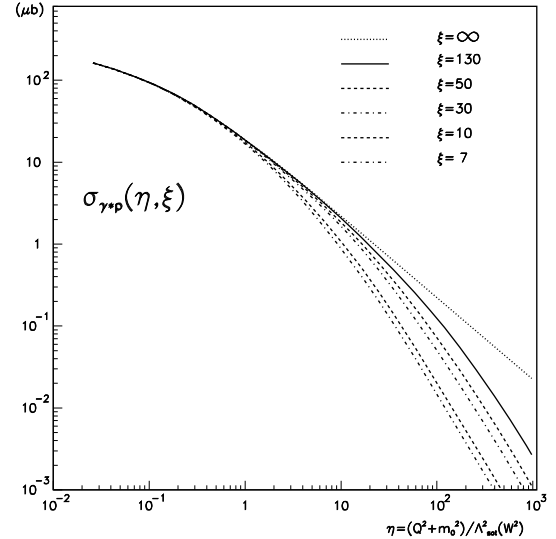


FIG. 1. The theoretical results for the photoabsorption cross section $\sigma_{\gamma^*p}(\eta(W^2, Q^2), \xi)$ in the CDP as a function of the low-x scaling variable $\eta(W^2, Q^2) = (Q^2 + m_0^2)/\Lambda_{sat}^2(W^2)$ for different values of the parameter ξ that determines the (squared) mass range $M_{q\bar{q}}^2 \leq m_1^2(W^2) = \xi\Lambda_{sat}^2(W^2)$ of the $\gamma^* \rightarrow q\bar{q}$ fluctuations that are taken into account. The experimental results lie on the full line corresponding to $\xi = 130$, compare refs. [1], [2].

energy-dependent upper bound on the $q\bar{q}$ mass, $M_{q\bar{q}} < m_1(W^2)$. In Fig. 1, reproduced from ref. [2], we show the theoretical prediction of the CDP for the photoabsorption cross section, $\sigma_{\gamma^*p}(W^2, Q^2)$, as a function of $\eta(W^2, Q^2)$ ⁴. The experimental data lie on the full line

* kurodam@law.meijigakuin.ac.jp

† schild@physik.uni-bielefeld.de

¹ Compare ref. [1] for an extensive list of references

² “Model-independent” means that the results for the photoabsorption cross section do not depend on an parameter-dependent explicit ansatz for the $q\bar{q}$ -dipole-proton interaction, except for a decent unitarity-preserving high-energy behavior.

³ The behavior in terms of $1/\eta(W^2, Q^2)$ is valid except for a logarithmic factor, $\sigma_{(q\bar{q})p}(W^2) \sim \ln W^2$ due to the dipole cross section $\sigma_{(q\bar{q})p}(W^2)$. See also the discussion on the relation of the dipole cross section to $(Q^2 = 0)$ photoproduction to be given below.

⁴ The curves in Fig. 1 are based on a fixed value of $W = 275 \text{ GeV}$. This is of importance due to the existence of a weak logarithmic, $\ln W$ -dependent violation of scaling in $\eta(W^2, Q^2)$ to be discussed later.

in Fig. 1, for an explicit representation including the experimental data compare e.g. ref. [1]. The different curves in Fig. 1 correspond to different upper bounds, $M_{q\bar{q}}^2 \lesssim m_1^2(W^2)$, parameterized by the constant ξ via $m_1^2(W^2) = \xi \Lambda_{sat}^2(W^2)$.

The experimental results obtained for $\eta(W^2, Q^2) > 10$, according to the full line in Fig. 1, require a finite value of $\xi \cong 130$, thus verifying the theoretical prediction from the CDP of the necessity of a W -dependent finite upper bound, $M_{q\bar{q}}^2 \leq m_1^2(W^2) = \xi \Lambda_{sat}^2(W^2)$.

For $\eta(W^2, Q^2) \lesssim 10$, however, the theoretical cross section for $\xi \rightarrow \infty$ ($m_1^2(W^2) \rightarrow \infty$) in good approximation coincides with the one for $\xi = 130$. In the kinematical region defined by $\eta(W^2, Q^2) \lesssim 10$, one can ignore the necessity for a finite upper bound on the mass of $q\bar{q}$ fluctuations. The usual treatment of the color-dipole approach, *without* introduction of an upper bound on the $q\bar{q}$ mass, $M_{q\bar{q}}$, given in the literature, in the hindsight can accordingly be justified by restricting the validity of these predictions to a finite kinematical region defined by $\eta(W^2, Q^2) \lesssim 10$.

The theoretical results for fixed values of $\xi < 130$ in Fig. 1 show a tendency to approach the results for $\xi = 130$ (or $\xi \rightarrow \infty$) for sufficiently small values of $\eta(W^2, Q^2) \ll 10$. This behavior indicates that with decreasing $\eta(W^2, Q^2)$ (or decreasing Q^2 at constant energy W) only $q\bar{q}$ states with a decreasing squared mass, $M_{q\bar{q}}^2 \leq \xi \Lambda_{sat}^2(W^2)$ with $\xi \ll 130$, are actually relevant in, or “active” for producing the cross section.

It is the purpose of this note to present a more detailed investigation of the mass range of $\gamma^* \rightarrow q\bar{q}$ fluctuations responsible for, or actively producing, the photoabsorption cross section, for different values of the kinematical variables W^2, Q^2 and $\eta(W^2, Q^2)$. We shall emphasize the different regions of $\eta(W^2, Q^2)$ related to color transparency and saturation. We comment on the impact of a future extension of the ep energy region, and on the extraction of the asymptotic energy dependence of ($Q^2 = 0$) photoproduction by extraction of the W -dependence of the dipole cross section.

II. THE MASS RANGE OF ACTIVE $q\bar{q}$ FLUCTUATIONS

For $\eta(W^2, Q^2) \gtrsim 10$, high-mass $q\bar{q}$ states, $M_{q\bar{q}}^2 \gtrsim \xi \Lambda_{sat}^2(W^2)$ where $\xi = 130$, do *not* contribute to the photoabsorption cross section. For $\eta(W^2, Q^2) \lesssim 10$, one may use $\xi \rightarrow \infty$ instead of $\xi = 130$, but actually, with decreasing $\eta(W^2, Q^2)$, according to Fig. 1, very massive states contribute a decreasing fraction to the photoabsorption cross section. We turn to an analysis to quantify the mass range of $q\bar{q}$ states that are responsible for the bulk of the cross section for $\eta(W^2, Q^2) \lesssim 10$.

Since in good approximation, for $\eta(W^2, Q^2) \lesssim 10$, the photoabsorption cross section for $\xi = 130$ coincides with the one for $\xi \rightarrow \infty$, see Fig. 1, we shall henceforth compare the cross section at any value of $\xi < 130$ with the one for $\xi \rightarrow \infty$ that for $\eta(W^2, Q^2) \lesssim 10$ is consistent with

experiment. Employing the expressions for the photoabsorption cross section as a function of $\eta(W^2, Q^2)$ and ξ in refs. [1, 2]⁵, a simple expansion in terms of $\eta/\xi \ll 1$ in leading order leads to a simple multiplicative factor to express the cross section for a given finite value of $\eta/\xi \ll 1$ in terms of the cross section for $\eta/\xi \rightarrow 0$,

$$\begin{aligned} \sigma_{\gamma^*p} \left(W^2, Q^2, \frac{\eta(W^2, Q^2)}{\xi} \right) = \\ \sigma_{\gamma^*p} \left(W^2, Q^2, \frac{\eta(W^2, Q^2)}{\xi} \rightarrow 0 \right) \\ \times \left(1 - \frac{3}{2} \frac{\eta(W^2, Q^2)}{\xi} \right). \end{aligned} \quad (1)$$

Equation (1), for $\eta(W^2, Q^2) \lesssim 10$, provides a simple representation of the dashed curves in Fig. 1 in terms of the full curve in Fig. 1.

We now want to find a procedure to quantify the range of masses $M_{q\bar{q}}^2 \leq m_1^2(W^2) = \xi \Lambda_{sat}^2(W^2)$ actually necessary to be taken into account to yield the experimentally measured cross section that for $\eta(W^2, Q^2) \lesssim 10$ coincides with the theoretical one for $\xi \rightarrow \infty$. To this end, we suggest to consider a deviation by a constant (i.e. $\eta(W^2, Q^2)$ -independent) fraction $\epsilon \ll 1$ from the experimentally measured cross section given by the theoretical result for $\xi \rightarrow \infty$ in Fig. 1.

From (1), we obtain the obvious condition

$$\begin{aligned} \sigma_{\gamma^*p} \left(W^2, Q^2, \frac{\eta(W^2, Q^2)}{\xi} \rightarrow 0 \right) (1 - \epsilon) = \\ \sigma_{\gamma^*p} \left(W^2, Q^2, \frac{\eta(W^2, Q^2)}{\xi} \rightarrow 0 \right) \\ \times \left(1 - \frac{3}{2} \frac{\eta(W^2, Q^2)}{\xi} \right). \end{aligned} \quad (2)$$

For any chosen value of $\epsilon \ll 1$, with decreasing $\eta(W^2, Q^2)$, a decreasing value of ξ , corresponding to a smaller upper limit of $m_1^2(W^2) = \xi \Lambda_{sat}^2(W^2)$ for $q\bar{q}$ states of squared mass $M_{q\bar{q}}^2$, is sufficient to yield a constant fraction of magnitude $(1 - \epsilon)$ of the photoabsorption cross section. Explicitly, from (2),

$$\xi = \frac{3}{2\epsilon} \eta(W^2, Q^2). \quad (3)$$

For e.g. $\epsilon = 0.1$, we have $\xi = 15\eta(W^2, Q^2)$. For any $\eta(W^2, Q^2) \lesssim 10$, from (3), we obtain a value of ξ that for e.g. $\epsilon = 0.1$ provides 90 % of the experimentally verified result for the photoabsorption cross section.

In terms of $m_1^2(W^2) = \xi \Lambda_{sat}^2(W^2)$, from (3), we have

$$\begin{aligned} m_0^2 \leq M_{q\bar{q}}^2 \leq m_1^2 = \frac{3}{2\epsilon} \eta(W^2, Q^2) \Lambda_{sat}^2(W^2) \\ = \frac{3}{2\epsilon} (Q^2 + m_0^2). \end{aligned} \quad (4)$$

⁵ Compare e.g. (2.36) in ref. [2].

TABLE I. The (η, W) matrix elements give the numerical values from (4) with $\epsilon = 0.1$ of the mass range $m_0 \leq M_{q\bar{q}} < m_1$ of $\gamma^* \rightarrow q\bar{q}$ transitions for fixed values of $\eta(W^2, Q^2) = (Q^2 + m_0^2)/\Lambda_{sat}^2(W^2)$ and energy W . At fixed η , with increasing energy W , increasing $q\bar{q}$ masses determine the cross section. At fixed W , with decreasing $\eta(W^2, Q^2)$ smaller masses determine the cross section.

| W [Gev] | 30 | 300 | 10 ⁴ |
|--------------------------------------|--|---|---|
| $\Lambda_{sat}^2(W^2)[\text{GeV}^2]$ | 1.95 | 6.75 | 44.8 |
| $\eta_{Min}(W^2)$ | 7.6×10^{-2} | 2.2×10^{-2} | 3.3×10^{-3} |
| $\eta = 1$ | $Q^2 = 1.8 \text{ GeV}^2$ $m_1^2 = 29 \text{ GeV}^2$ $m_1 = 5.4 \text{ GeV}$ | $Q^2 = 6.9 \text{ GeV}^2$ $m_1^2 = 101 \text{ GeV}^2$ $m_1 = 10 \text{ GeV}$ | $Q^2 = 44.7 \text{ GeV}^2$ $m_1^2 = 672 \text{ GeV}^2$ $m_1 = 25 \text{ GeV}$ |
| $\eta = 0.1$ | $Q^2 = 4.5 \times 10^{-2}$ $m_1^2 = 2.9 \text{ GeV}^2$ $m_1 = 1.7 \text{ GeV}$ | $Q^2 = 0.53 \text{ GeV}^2$ $m_1^2 = 10.1 \text{ GeV}^2$ $m_1 = 3.2 \text{ GeV}$ | $Q^2 = 4.3 \text{ GeV}^2$ $m_1^2 = 67 \text{ GeV}^2$ $m_1 = 8.2 \text{ GeV}$ |
| $\eta = \eta_{Min}$ | | $Q^2 = 0$ $m_1^2 = 2.25 \text{ GeV}^2$ $m_1 = 1.5 \text{ GeV}$ | |

For any W^2 and Q^2 with $\eta(W^2, Q^2) \lesssim 10$, the constraint (4) determines the mass range of $q\bar{q}$ dipole states that are essential for the cross section in the sense of providing a (large) fraction of magnitude $1 - \epsilon$ of the photoabsorption cross section $\sigma_{\gamma^*p}(W^2, Q^2)$. In other words, the dominant contribution to the photoabsorption cross section for fixed $\eta(W^2, Q^2) \lesssim 10$ is due to $q\bar{q}$ states that have masses below the limit given in (4). The masses of these “active” $q\bar{q}$ states are restricted by the value of the photon virtuality Q^2 according to (4). A fixed value of Q^2 is uniquely associated with a fixed $q\bar{q}$ dipole-mass range.

In Table I, for the choice of $\epsilon = 0.1$, we show the results of a numerical evaluation of the upper limit m_1^2 from (4) for various values of $\eta(W^2, Q^2) \lesssim 10$ and for energies in the range of $W \lesssim 300 \text{ GeV}$ explored at HERA [3], and at the energy $W = 10^4 \text{ GeV}$ recently discussed in view of future collider projects [4]. For the saturation scale $\Lambda_{sat}^2(W^2)$, and for m_0^2 , we use the parameters adjusted⁶ to the experimental data from HERA for $x_{bj} \cong Q^2/W^2 \lesssim 0.1$, i.e.

$$\Lambda_{sat}^2(W^2) = C_1 \left(\frac{W^2}{1 \text{ GeV}^2} \right)^{C_2} = 0.31(W^2)^{0.27},$$

$$m_0^2 = 0.15 \text{ GeV}^2. \quad (5)$$

According to Table I, for various fixed values of $\eta(W^2, Q^2)$, with increasing W , we find the expected increase of the upper limit for relevant $q\bar{q}$ states, $M_{q\bar{q}}^2 \lesssim m_1^2$. For e.g. $\eta(W^2, Q^2) = 1$, we have $M_{q\bar{q}}^2 \leq m_1^2 = 29 \text{ GeV}^2$ at $W = 30 \text{ GeV}$, and $M_{q\bar{q}}^2 \leq m_1^2 = 101 \text{ GeV}^2$ at

TABLE II. The (Q^2, W) matrix elements are the values of $\eta(W^2, Q^2) = (Q^2 + m_0^2)/\Lambda_{sat}^2(W^2)$. A fixed value of Q^2 is associated with a fixed (squared) mass range, $m_0^2 \leq M_{q\bar{q}}^2 \leq m_1^2$. With increasing energy W , for fixed $M_{q\bar{q}}^2 < m_1^2$, the transition from color transparency ($\eta \gg 1$) to saturation ($\eta \ll 1$) takes place. For $Q^2 \simeq 0$, hadronlike saturation behavior occurs for all values of W shown. With decreasing Q^2 at fixed W decreasing masses, $M_{q\bar{q}}^2 < m_1^2$ determine the cross section.

| W [Gev] | 30 | 300 | 10 ⁴ |
|---|----------------------|----------------------|----------------------|
| $\Lambda_{sat}^2(W^2)[\text{GeV}^2]$ | 1.95 | 6.75 | 44.8 |
| $Q^2 = 10 \text{ GeV}^2$ $m_1^2 = 152 \text{ GeV}^2$ $m_1 = 12.3 \text{ GeV}$ | 5.2 | 1.5 | 2.3×10^{-1} |
| $Q^2 = 2 \text{ GeV}^2$ $m_1^2 = 32.3 \text{ GeV}^2$ $m_1 = 5.68 \text{ GeV}$ | 1.1 | 3.2×10^{-1} | 4.8×10^{-2} |
| $Q^2 = 0$ $m_1^2 = 2.25 \text{ GeV}^2$ $m_1 = 1.5 \text{ GeV}$ | 7.7×10^{-2} | 2.2×10^{-2} | 3.3×10^{-3} |

$W = 300 \text{ GeV}$, and finally $M_{q\bar{q}}^2 \leq m_1^2 = 672 \text{ GeV}^2$ at $W = 10^4 \text{ GeV}$. With decreasing $\eta(W^2, Q^2)$ at fixed W , the decrease in Q^2 is accompanied by a decrease in m_1^2 , leading to $M_{q\bar{q}}^2 \leq m_1^2 = 2.25 \text{ GeV}^2$ at $\eta(W^2, Q^2) = \eta(W^2, Q^2 = 0) \equiv \eta_{Min}$. It is amusing to note that the value of $m_1 = 1.5 \text{ GeV}$ practically coincides with the value of $m_1 = 1.4 \text{ GeV}$ from the 1972 Generalized Vector Dominance (GVD) interpretation [5] of the first data on DIS from the SLAC-MIT collaboration [6].

In Table II, we present the values of the scaling variable $\eta(W^2, Q^2)$ corresponding to fixed values of Q^2 (and of m_1^2 according to (4) with $\epsilon = 0.1$), for different values of W chosen as in Table I. The Table illustrates that an identical fixed mass range, defined by $m_0^2 \leq M_{q\bar{q}}^2 \leq m_1^2$, is responsible for cross sections in the color transparency region and the saturation region; e.g. for $Q^2 = 2 \text{ GeV}^2$ and $m_1 = 5.68 \text{ GeV}$, we see the transition from $\eta = 1.1 \gtrsim 1$ at $W = 30 \text{ GeV}$ to $\eta = 4.8 \times 10^{-2} \ll 1$ that is reached at $W = 10^4 \text{ GeV}$. As a consequence of the two-gluon color-dipole interaction, a massive $q\bar{q}$ state of mass $M_{q\bar{q}}$, dependent on the energy W , either interacts with a small cross section (color transparency), $\sigma_{\gamma^*p}(W, Q^2) \sim 1/\eta(W^2, Q^2)$, or with a moderately large one, $\sigma_{\gamma^*p}(W^2, Q^2) \sim \ln(1/\eta(W^2, Q^2))$.

So far in this paper, we have been concerned with the interpretation of the photoabsorption cross section as a function of the low-x scaling variable $\eta(W^2, Q^2)$ in terms of the relevant $q\bar{q}$ dipole masses, $M_{q\bar{q}}$, of $\gamma^* \rightarrow q\bar{q}$ transitions. For the last part of this work, we recall that the dependence of the photoabsorption cross section on $\eta(W^2, Q^2)$, as mentioned in footnote 4, is actually weakly violated by a logarithmic W dependence of the

⁶ Compare e.g. (3.10) in ref. [2]

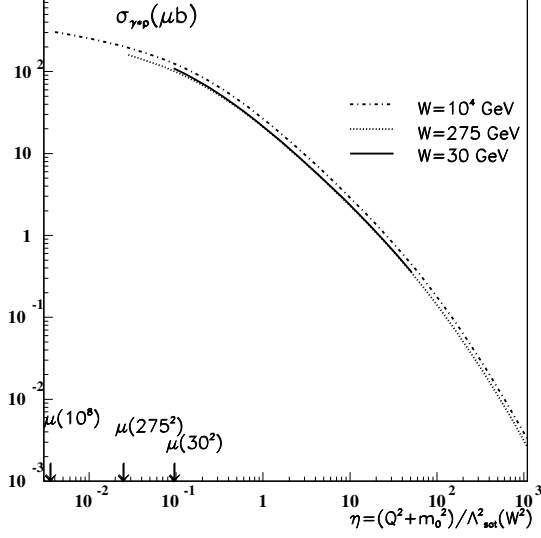


FIG. 2. The theoretical results for the photoabsorption cross section as a function of $\eta(W^2, Q^2)$ for different values of W . The dependence on W is due to logarithmic η -scaling violations due to $\sigma^{(\infty)}(W^2) \sim \ln W^2$ in (6). For ξ the value $\xi = 130$ is used, and the results for $W = 275$ GeV are identical to the results shown by the full curve in Fig. 1. By definition, $\mu(W^2) \equiv m_0^2/\Lambda_{sat}^2(W^2)$.

dipole cross section, $\sigma_{(q\bar{q})p}(W^2) \equiv \sigma^{(\infty)}(W^2) \sim \ln(W^2)$. Putting $\xi \rightarrow \infty$, the photoabsorption cross section is given by (e.g. (2.17) in ref. [2])

$$\sigma_{\gamma^*p}(W^2, Q^2) = \frac{\alpha R_{e^+e^-}}{3\pi} \sigma^{(\infty)}(W^2) I_0(\eta(W^2, Q^2)). \quad (6)$$

Here, $R_{e^+e^-} = 3\Sigma_q Q_q^2$, where the sum runs over the actively contributing quark charges. Concerning the function $I_0(\eta(W^2, Q^2))$, for the present purpose, it is sufficient to note the leading behavior for $\eta(W^2, Q^2) \rightarrow \eta_{Min}(W^2) \ll 1$,

$$I_0(\eta) \cong \ln(1/\eta(W^2, Q^2)). \quad (7)$$

In order to assure a smooth transition to $Q^2 = 0$ photoproduction, $\sigma_{\gamma p}(W^2)$, the dipole cross section in (6), employing (7), must be related to $\sigma_{\gamma p}(W^2)$ by

$$\sigma^{(\infty)}(W^2) = \frac{3\pi}{\alpha R_{e^+e^-}} \frac{1}{\ln \frac{\Lambda_{sat}^2(W^2)}{m_0^2}} \sigma_{\gamma p}(W^2), \quad (8)$$

and (6) becomes

$$\begin{aligned} \sigma_{\gamma^*p}(W^2, Q^2) &= \frac{\sigma_{\gamma p}(W^2)}{\ln \frac{\Lambda_{sat}^2(W^2)}{m_0^2}} I_0(\eta(W^2, Q^2)) \\ &\xrightarrow{Q^2 \rightarrow 0} \sigma_{\gamma p}(W^2). \end{aligned} \quad (9)$$

For an asymptotic behavior of $\sigma_{\gamma p}(W^2) \sim (\ln W^2)^2$, the dipole cross section in (8) must have the above-mentioned

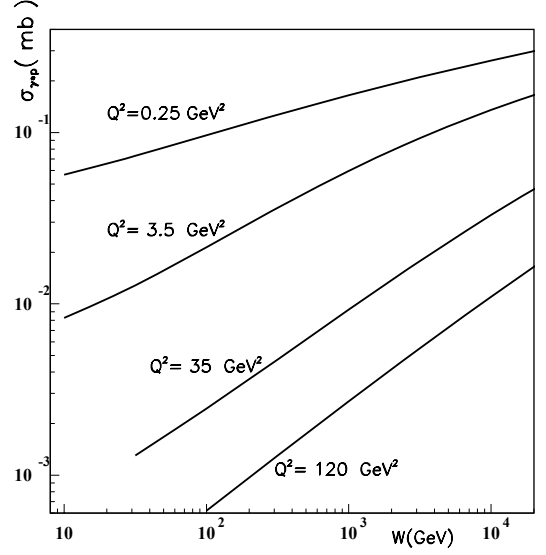


FIG. 3. The photoabsorption cross section as a function of the energy W for different values of Q^2 . Note that a fixed value of Q^2 is associated with a fixed mass range of $q\bar{q}$ dipole states, $M_{q\bar{q}} \leq m_1$ as determined by (4). Compare also Table II. Transition from color transparency to saturation at fixed Q^2 is a consequence of the two-gluon coupling of the $q\bar{q}$ dipole state.

logarithmic increase, $\sigma^{(\infty)}(W^2) \sim \ln W^2$. Assuming $\sigma_{\gamma p}(W^2) \sim (\ln W^2)^2$, in Fig. 2, according to (6), we supplement the results in Fig. 1 for $W = 275$ GeV by the results at $W = 30$ GeV and 10^4 GeV.

In Fig. 3, we show the photoabsorption cross section for fixed values of Q^2 as a function of W . Since Q^2 is fixed, from (4), also the range of $q\bar{q}$ masses is fixed. From (9), we have the well-known result [7] of

$$\lim_{\substack{W \rightarrow \infty \\ Q^2 > 0 \text{ fixed}}} \frac{\sigma_{\gamma^*p}(W^2, Q^2)}{\sigma_{\gamma p}(W^2)} = 1. \quad (10)$$

Inverting (8),

$$\sigma_{\gamma p}(W^2) = \frac{\alpha R_{e^+e^-}}{3\pi} \ln \left(\frac{\Lambda_{sat}^2(W^2)}{m_0^2} \right) \sigma^{(\infty)}(W^2), \quad (11)$$

we now draw an important conclusion concerning the extraction of the total ($Q^2 = 0$) *photoproduction* cross section from the DIS experimental data on $\sigma_{\gamma^*p}(W^2, Q^2)$ according to (6). The experimental data at fixed energy W under variation of Q^2 are expected to yield results lying on the associated curve on the η -plot in Fig. 2. In particular, a fit yields experimental results for $\sigma^{(\infty)}(W^2)$, and accordingly experimental results for $\sigma_{\gamma p}(W^2)$ upon substitution of the experimental results for $\sigma^{(\infty)}(W^2)$ into (11). Note that this two-step procedure to determine $\sigma_{\gamma p}(W^2)$ does not rely on measurements close to $Q^2 \sim 0$, and on an ad hoc extrapolation to $Q^2 = 0$.

We discuss two cases: If the experimental data in Fig. 2 lie on a single line, we have $\sigma^{(\infty)}(W^2) = const.$ and,

accordingly, $\sigma_{\gamma p} \sim \ln(W^2)$. For the case of $\sigma^{(\infty)}(W^2) \sim \ln(W^2)$, we have $\sigma_{\gamma p}(W^2) \sim (\ln(W^2))^2$, as shown by the theoretical curves in Fig. 2. An energy extension to e.g. $W \sim 10^4$ GeV, allows one to contribute to answering the important question on whether the total *photoproduction* cross section asymptotically behaves hadronlike, $\sigma_{\gamma p} \sim (\ln(W^2))^2$. A $(\ln W^2)^2$ behavior of the cross section for hadron-hadron scattering was first predicted by Heisenberg [8], and later, by Froissart [9] from analyticity arguments, was shown to coincide with the maximally allowed growth of hadronic cross sections with energy.

III. CONCLUSIONS

The present work is concerned with an interpretation of the photoabsorption cross section in terms of the range of the masses $M_{q\bar{q}}$ of $\gamma^* \rightarrow q\bar{q}$ fluctuations that actively contribute to this cross section. The essential result is contained in (4). The mass range of active $q\bar{q}$ fluctuations is uniquely determined by a proportionality to the photon virtuality Q^2 . At fixed $Q^2 \geq 0$, it is a fixed range of

dipole masses that, as a consequence of the two-gluon $q\bar{q}$ dipole coupling, with sufficient increase of the energy W leads to the observed transition from color transparency, $\sigma_{\gamma^* p}(\eta(W^2, Q^2)) \sim 1/\eta(W^2, Q^2)$ for $\eta(W^2, Q^2) \gg 1$, to saturation, $\sigma_{\gamma^* p}(\eta(W^2, Q^2)) \sim \ln(1/\eta(W^2, Q^2))$ for $\eta(W^2, Q^2) \ll 1$. Alternatively, at fixed energy W , a sufficient decrease in Q^2 towards $Q^2 \cong 0$, associated with a decrease of the mass range of active fluctuations, also leads from $\eta(W^2, Q^2) \gg 1$ (color transparency) to $\eta(W^2, Q^2) \ll 1$ (saturation). Even though for $Q^2 > 0$ fixed, the active $q\bar{q}$ fluctuations have a larger mass than at $Q^2 = 0$, in the true limit of $W \rightarrow \infty$ the ratio of the cross section at fixed $Q^2 > 0$, to the $Q^2 = 0$ photoproduction cross section converges towards unity.

The low-x scaling of the photoabsorption cross section in $\eta(W^2, Q^2)$ is weakly violated by a $\ln W^2$ dependence due to the dipole cross section, $\sigma^{(\infty)}(W^2) \sim \ln W^2$. The extraction of this W-dependence of the dipole cross section from the Q^2 dependence of DIS electron-proton scattering at different energies W (not necessarily including values of Q^2 close to $Q^2 \approx 0$) allows one to extract the $Q^2 = 0$ photoproduction cross section and to verify or falsify its hadronlike $(\ln W^2)^2$ dependence.

-
- [1] M. Kuroda and D. Schildknecht, *Phys. Rev. D* **85**, 094001 (2012).
 - [2] M. Kuroda and D. Schildknecht, *Int. Journal of Mod. Phys. A* **31**, 1650157 (2016).
 - [3] H1 Collaboration, *Eur. Phys. J. C* **74**, 281 (2014); ZEUS Collaboration, *Phys. Rev. D* **90** 072002 (2014).
 - [4] A. Caldwell and M. Wing, arXiv: 1606.00783.
 - [5] J.J. Sakurai and D. Schildknecht, *Phys. Lett. B* **40**, 121 (1972).
 - [6] SLAC-MIT collaboration, G. Miller et al., *Phys. Rev D* **5**, 528 (1972).
 - [7] D. Schildknecht, *Nucl. Phys. Proc. Suppl.* **99A**, 121 (2001).
 - [8] W. Heisenberg, *Vorträge über kosmische Strahlung* (Springer, Berlin, 1953), p. 155, reprinted in *W. Heisenberg, Collected Works*, Series B (Springer, Berlin, 1984) p. 498; W. Heisenberg, *Die Naturwissenschaften* **61** (1974), 1, reprinted in *Collected Works*, Series B, p. 912.
 - [9] M. Froissart, *Phys. Rev.* **123**, 1053 (1961).